The $^1\Delta_g$ Dioxygen Ene Reaction with Propene: A Density Functional and Multireference Perturbation Theory Mechanistic Study

Andrea Maranzana, Giovanni Ghigo, and Glauco Tonachini*[a]

Abstract: This study aims to determine whether a balance between concerted and non-concerted pathways exists, and in particular to ascertain the possible role of diradical/zwitterion or peroxirane intermediates. Three non-concerted pathways, via 1) diradical or 2) peroxirane intermediates, and 3) by means of hydrogen-abstraction/radical recoupling, plus one concerted pathway (4), are explored. The intermediates and transition structures (TS) are optimized at the DFT(MPW1K), DFT(B3LYP) and CASSCF levels of theory. The latter optimizations are followed by multireference perturbative CASPT2 energy calculations. 1) The polar diradical forms from the separate reactants by surmounting a barrier ($\Delta E^{\ddagger}_{MPW1K} = 12$, $\Delta E^{\ddagger}_{B3LYP} = 14$, and $\Delta E^{\ddagger}_{CASPT2} =$ 16 kcal mol^{-1} and can back-dissociate through the same TS, with barriers of 11 (MPW1K) and 8 kcal mol^{-1} (B3LYP and CASPT2). The diradical to hydroperoxide transformation is easy at all levels ($\Delta E^{\ddagger}_{MPW1K} < 4$, $\Delta E^{\ddagger}_{B3LYP} = 1$ and $\Delta E^{\ddagger}_{CASPT2} = 1$ kcal mol^{-1}). 2) Peroxirane is attainable only by passing through the diradical intermediate, and not directly, due to the nature of the critical points involved. It is located higher in energy than the diradical by 12 kcal mol^{-1}, at all theory levels. The energy barrier for the diradical to *cis*-peroxirane transformation ($\Delta E^{\ddagger} = 14$–16 kcal mol^{-1}) is much higher than that for the diradical transformation to the hydroperoxide. In addition, peroxirane can very easily back-transform to the diradical ($\Delta E^{\ddagger} < 3$ kcal mol^{-1}). Not only the energetics, but also the qualitative features of the energy hypersurface, prevent a pathway connecting the peroxirane to the hydroperoxide at all levels of theory. 3) The last two-step pathway (hydrogen-abstraction by $^1O_2$, followed by HOO-allyl radical coupling) is not competitive with the diradical mechanism. 4) A concerted pathway is carefully investigated, and deemed an artifact of restricted DFT calculations. Finally, the possible ene/[π2+π2] competition is discussed.

Keywords: ab initio calculations · density functional calculations · ene reaction · reaction mechanisms · singlet oxygen

Introduction

$^1\Delta_g$ is the first excited state of dioxygen, degenerate, and 22.5 kcal mol^{-1} higher than the ground state triplet ($^3\Sigma^+_g$). As a reactive species in oxidation reactions[1, 2a] it is important and ubiquitous. It can be generated in the troposphere by ozone photolysis,[2b, 3] or by the oxidation and combustion of hydrocarbons (autoxidation).[2c, 4a] It can also be prepared in the laboratory by chemical (and photochemical) techniques.[2a, 2d, 5a] Both useful and destructive, it has been exploited for synthetic purposes,[2a] while its reactions with some biomolecules have been investigated,[2e] so establishing that it is capable of attacking DNA bases,[5b] and, by and large, of damaging organic tissues.

[a] Prof. G. Tonachini, A. Maranzana, G. Ghigo
Dipartimento di Chimica Generale e Organica Applicata
Università di Torino
Corso Massimo D'Azeglio 48, 10125 Torino (Italy)
Fax: (+39) 11-670-7642
E-mail: glauco.tonachini@unito.it

Supporting information for this article is available on the WWW under http://www.chemeurj.org/ or from the author.

$^1\Delta_g$ O_2 exhibits a diverse reactivity with organic unsaturated molecules,[6–8] as shown in Scheme 1, where the three main modes of attack are displayed. Two cycloadditions are possible, the [π2+π2] addition to one C=C double bond, that produces a 1,2-dioxetane, and the [π4+π2] addition, which is possible if the substrate is a conjugated (s-*cis*) diene, and generates an endoperoxide.

If one allylic hydrogen is available, another channel is open, and a hydroperoxide can form. This is called the *ene*[9] (Schenck)[10, 11] reaction, and is the subject of the present investigation. It is not necessary for the hydrogen to be allylic for the abstraction to take place. In fact, it has recently been reported that a vinyl hydrogen atom, rather than allyl hydrogen atom, is preferentially abstracted in highly twisted 1,3-dienes to give allenes (in a diastereoselective way).[12] The addition to phenol derivatives (Scheme 1) is a reaction similar to the ene, and yields hydroperoxide ketones.[13, 15] The ene reaction, although to some extent resembling the [π4+π2] reaction, is not a cycloaddition, but a group transfer reaction.[14] The different reactions can compete, if the substrate structure allows it. For instance, dioxetane formation is found to prevail over hydroperoxide formation with electron-rich

DOI: 10.1002/chem.200204522

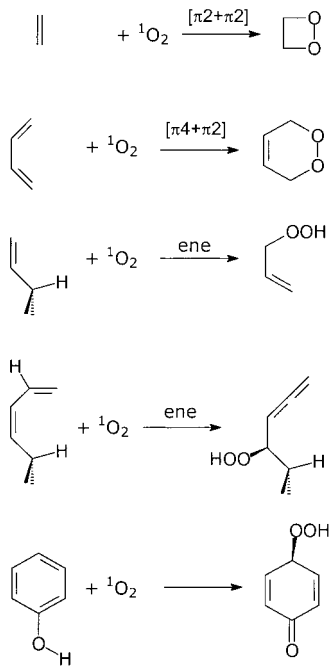

Scheme 1. Reactions of $^1\Delta_g$ O_2 with organic unsaturated molecules.

alkenes, whilst electron-withdrawing substituents promote the ene mode.[16]

A large number of experiments have been carried out in an attempt to elucidate the mechanistic features of the singlet oxygen reactions. The mechanisms of the three mentioned reactions are in fact related by the possibility of sharing the intermediacy of some short-lived structure.[7, 11] Both two-step and concerted mechanisms have been proposed for the ene reaction. On the basis of the experimental evidence collected on different molecular systems, divergent reaction mechanisms have been proposed so far,[7, 8] and no ultimate answer seems to be available at the present.

Concerted and non-concerted modes of attack are sketched in Scheme 2 for the ene reaction (conceivable channels represented by dashed arrows). The non-concerted pathways might involve either open-chain diradical/zwitterionic intermediates, or a cyclic peroxirane intermediate (also called perepoxide). The concerted pathways would require the formation of one C–O bond, accompanied, in the same kinetic step, by a methyl hydrogen transfer to the other oxygen atom. A further channel could consist of a first hydrogen-abstraction step (operated by O_2), followed by radical recombination to give the hydroperoxide.

Some evidence has been collected in favor of the existence of non-concerted pathways in the ene reaction (and in the [π2+π2] reaction).[6b] In particular, a series of stereochemical studies,[11, 17, 18] as well as kinetic isotope effect (KIE) experiments concerning the ene reaction[19–22] have yielded results that are apparently best accommodated by the intermediacy of peroxirane, or a peroxirane-like exciplex. Solvent polarity effects have led some researchers to postulate the intervention either of more or less loosely structured exciplexes, or of peroxiranes, not only for the ene mode, but also for the [π2+π2] and the [π4+π2] reactions.[11, 16, 18, 23–25] Evidence for the intervention of a peroxirane species in [π2+π2] cycloadditions is somewhat less persuasive than for the ene reaction,[15, 28–31] although the ene pathway seems to be less polar than the pathway for dioxetane formation (this has been inferred from the observation that dioxetane formation can be enhanced by an increase in solvent polarity, and can become the preferential pathway, or even the only one).[15, 18–20] In fact, some indications for the involvement of open-chain zwitterion intermediates are also given in the literature.[26, 27]

The contribution of theoretical investigations carried out by other researchers has flanked the experimental efforts to elucidate the ene and [π2+π2] reaction mechanisms. Earlier semiempirical investigations[32] suggested that a peroxirane could play an important role, but indicated for electron-rich alkenes, the likely intermediacy of an open-chain zwitterion. By contrast, successive GVB – CI calculations were in favor of a diradical mechanism, and determined for peroxirane an energy higher than that of the diradical.[33] Further ab initio and semiempirical UHF calculations led to the same description, but the authors were induced to suggest a concerted mechanism by the computationally predicted and experimentally observed stereospecificity and regioselectivity.[34]

A CCI and CASSCF study based on symmetry-constrained geometry optimizations defined the C_s peroxirane "pathway" as easier than that involving a C_s (*syn*) diradical.[35] Information on lower symmetry pathways was not available, and it was not possible to determine whether the C_s critical points were authentic transition structures, because of the symmetry constraints. Evidence in favor of the formation of diradical

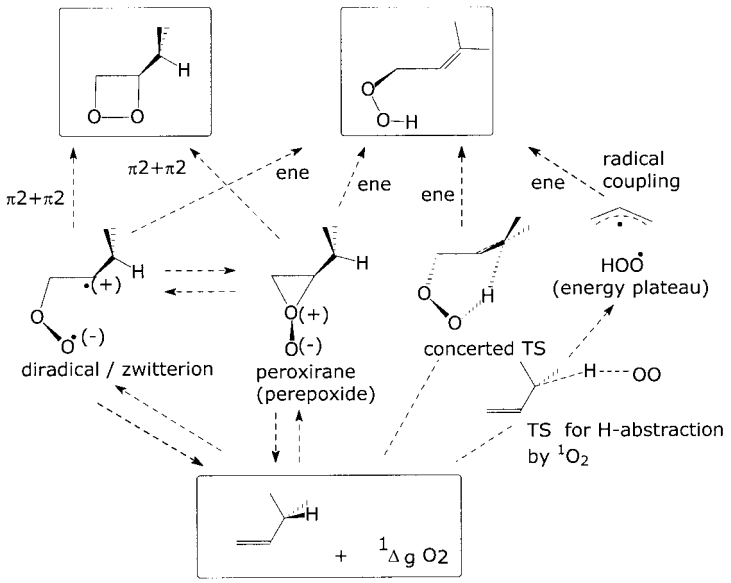

Scheme 2. Concerted and nonconcerted reaction pathways for the ene reaction.

intermediates was derived from CASSCF studies on ethene[36, 37] and ethenol,[38] by using fully unrestricted geometry optimizations. Peroxirane structures were found to correspond to energy minima on the energy surfaces, but these structures were attainable only by passing first through the open-chain diradical intermediates. A diradical intermediate was also found in a recent CAS–MC–QDPT2 and CASSCF study of the [π4+π2] cycloaddition of singlet oxygen to butadiene. (On the other hand the addition to benzene was found to take place in a concerted fashion.[39])

Herein we discuss the reaction of singlet dioxygen with propene, the simplest alkene system capable in principle of undergoing the ene reaction. This study is limited to this model molecule because of the number of different tests carried out on several aspects of the reactivity. However, other more substituted systems are currently being examined, because other interesting aspects can be related to the presence of more than one substituent on the double C=C bond. The aim of the study described herein is to contribute to the understanding of the relative importance of concerted and non-concerted pathways leading to the hydroperoxide product in the gas phase, and to assess the relevant barrier heights. The potential competition of the ene reaction with the [π2+π2] cycloaddition is also discussed. The possible intermediacy of diradical and peroxirane species, as well as their interconversion and competition, will be discussed. Accordingly, the distinction between a zwitterion and a diradical must not be perceived as too rigid, because a carbon–oxygen diradical is endowed with some zwitterionic character.[40] Although, in the present case, gas-phase calculations show that a more pronounced zwitterionic character is pertinent to excited electronic states of the same open-chain molecules, polar diradicals (as those found in this study) can be considered as representative of pathways involving open-chain intermediates.

Methods

The study of the model reaction was carried out by determining the critical points and the related energy differences on the gas-phase reaction energy hypersurface. Two different theoretical methods (A and B, here below) were used, and the polarized 6–311G(d,p) basis set[41] was used throughout the study.

Method A) The geometrical structures of the critical points were optimized without constraints by gradient methods[42] at the complete active space multi-configuration self-consistent field level of theory (CAS–MCSCF, hereafter CASSCF).[43] To better assess the energy difference estimates, dynamic correlation effects were then taken into account through CASPT2 calculations, that is by multireference second-order perturbation theory (PT2), for which the reference wavefunction Ψ_0 is the CASSCF wavefunction.[44] Both the MCSCF and PT2 computations require the definition of the active space of orbitals, within which every possible electron promotion is taken into account (complete active space, CAS), thus providing the complete CI that defines Ψ_0. The active space chosen for the geometry optimization of the separate reactants includes: I) the π system of propene (π_{CC} and π^*_{CC}); II) a σ_{CH}, σ^*_{CH} couple of orbitals pertaining to the C–H bond involved in the hydrogen transfer to oxygen; III) the two π_u and the two π_g orbitals of O_2; IV) the σ_{OO}, σ^*_{OO} orbitals of O_2. This choice is shown in Scheme 3.

In the final set of single-point CASSCF and CASPT2 (frozen core) calculations, which were carried out to better assess the relative energies, a uniform larger active space was chosen for all structures.

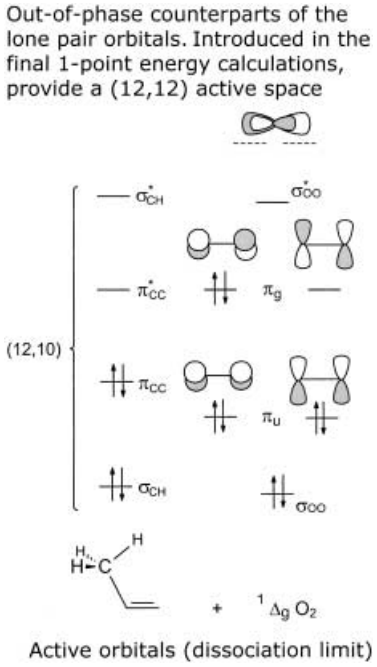

Scheme 3.

This active space additionally includes two orbitals, incorporated as "empty counterparts" of the oxygen lone-pair orbitals, to improve convergence. These are sketched by the dashed lines shown in Scheme 3. Each one of these is similar to the lone pair orbitals, but has out-of-phase contributions on the oxygen atoms involved, whereas the lone pair orbital has in-phase contributions.

The eight-orbital set (I–III), populated by ten electrons in all possible ways, defines the "ten electrons in eight orbitals" CAS, labeled as (10,8), while the more extended active space (I–IV) defines the "twelve electrons in ten orbitals" active space, (12,10). The electron configuration shown in Scheme 3, and that obtained by shifting the two π_g electrons into the rightmost π_g orbital (with equal weights and combined with the minus sign) define one of the two degenerate $^1\Delta_g$ electronic states of the O_2 molecule. If one of the two π_g electrons is assigned to the leftmost and the other to the rightmost π_g orbital, the two-determinant configuration that dominates the second degenerate $^1\Delta_g$ electronic state is obtained. As the alkene and O_2 approach each other, other configurations can contribute significantly to the CI eigenvector, as a function of the geometry of approach. Therefore, depending on the structure under scrutiny, two oxygen lone pairs are found associated to different orbitals.

Both the (10,8) and (12,10) active spaces were used to optimize all the stable and transition structures discussed in the next section. The nature of the critical points, qualified as energy minima or saddle points (of first or higher order) could be determined by vibrational analysis only at the (10,8) level, at which the computation of the analytic Hessian was feasible. The same (10,8) computations provided thermochemical information. The geometries obtained with the two active spaces show insignificant changes, with the exception of the O–O bond length, that is obviously sensitive to the extension of the active space to the σ_{OO}, σ^*_{OO} orbital pair. In the final set of single-point CASPT2 calculations, the uniform larger active space chosen for all structures has the (12,10) space as a basis, plus the two "empty counterparts" of the oxygen lone-pairs orbitals sketched in Scheme 3. This choice defines a (12,12) active space. From these homogeneous energies, the energy differences reported in Table 1 were obtained. The enthalpy and free energy estimates are obtained by adding the relevant corrections computed at the (10,8) level (also collected in Table 1). The exclusion of the σ_{OO} and σ^*_{OO} orbitals in going from the (12,10) to the (10,8) active space could affect the thermochemical estimates in a non-negligible way; thus, they should be considered with due caution. The full set of energies at the various computational levels is presented in the Supporting Information, together with the optimized geometrical parameters of the critical points.

Method B) The stable and transition structures were determined by gradient procedures[45] within density functional theory (DFT),[46a,b] making use of the B3LYP[46c] and MPW1K[46d] functionals and the 6–311G(d,p) basis set. The former functional is very popular and of widespread use, and, even if prone to underestimate some reaction barriers, has generally performed well as regards geometries and energetics. The latter functional has been more recently defined with the aim of obtaining reliable energy barriers.

One problem arises because the unrestricted DFT (UDFT) calculations on diradical species converge on closed-shell type solutions, with zero spin densities (i.e. the unrestricted framework produces a restricted solution). This obviously gives an incorrect description of diradical or diradicaloid structures. To get a qualitatively correct description, two highest occupied/lowest unoccupied orbital rotations are switched on, right from the beginning of the iterative SCF-like procedure, one within the α set, the other within the β set. The qualitative description of a diradical or diradicaloid species, after convergence, is satisfactory in terms of nonzero spin densities, and is thus likely to generate reasonable structures. Yet, this handling of the UDFT monodeterminantal wavefunction gives rise to a significant spin contamination by the triplet in the wavefunction itself, as evidenced by the $\langle \hat{S}^2 \rangle$ values, which may yield a value close to 1. Therefore, the nature of the wavefunction is intermediate between the singlet and triplet spin multiplicities, and the energy values so obtained need to be refined by some spin-projection method to eliminate the spin contaminants. This was accomplished in an approximate way by using the formula suggested by Yamaguchi et al.,[47a] that allows elimination of the largest contaminant of the singlet, i.e., the triplet.[47b]

When two species react to form an adduct, the basis set superposition error (BSSE)[46e] can affect the energy differences. Due to the indirect and somewhat elaborate procedure just mentioned we preferred to assess the effect of a basis set extension instead of estimating the BSSE. This effect was then explored by a couple of tests carried out at the MPW1K level only. All the energies were initially recomputed by the 6–311G(3df,2p) basis set, in conjunction with the 6–311G(d,p) optimum geometries. Then for three selected points (the dissociation limit, the diradical formation TS, and the diradical), whose energy differences could be particularly affected by a BSSE, single-point energy calculations were carried out with the larger aug–cc–pVTZ basis set of Dunning.[41b] In all cases the variations are moderate (as can be seen from Table 2).

Method C) The condensed phase simulation was carried out at the DFT(B3LYP) level by using the self-consistent reaction field (SCRF) approach,[48a] in conjunction with two methods. One is based on the use of the Onsager–Kirkwood model[48b] for single-point calculations, in which the order of multipole used is the hexadecapole. The other is the polarized continuum model (PCM) method, put forward by Tomasi and co-workers, with and without geometry re-optimization.[48c] The solvents considered were $CHCl_3$ and CH_3CN.

The DFT and CASSCF optimizations were carried out by using the GAUSSIAN 98 system of programs.[49] The natural bond orbital (NBO) analysis,[50] implemented in that suite, was used to evaluate the natural atomic orbital (NAO) charges. The CASSCF and CASPT2 calculations with the largest active space were done with the MOLCAS4 program.[51] The two transition structures shown in the Figures 1 and 7 are drawn by the MolMol 2.4[52] program.

Results and Discussion

The results pertaining to the gas-phase mechanism are presented and discussed in this section (ΔE, ΔH, and ΔG values, relative to the separated propene and singlet dioxygen reagents **1**, are collected in Table 1 and Table 2), and are followed at the end by a brief comment on some condensed phase results.

Table 1. CASPT2(12,12) relative energies, and estimates of the enthalpy and free energy differences[a] (at 298 K).

Structure		ΔE	ΔH[b]	ΔG[b]
propene + $^1\Delta_g$ O_2	**1**	0.0	0.0	0.0
diradical formation	**TS 1–2a**	15.7	15.9	26.1
peroxyl diradical	**2a**	7.1	9.0	19.0
diradical to hydroperoxide	**TS1–3**	*0.6*	*7.8*	*20.0*
hydroperoxide	**3**	−33.4	−30.1	−19.9
diradical to peroxirane	**TS3–4**	22.3	23.3	35.0
peroxirane	**4**	19.5	22.3	33.5
hydrogen abstraction	**TS1–5**	33.6	30.4	38.6
HOO + allyl radicals	**5**	18.7	16.5	14.3
diradical to dioxetane	**TS2a–6**	17.8	19.0	30.0
dioxetane	**6**	−29.9	−25.9	−14.7

[a] In kcal mol^{-1} (see text for details). [b] The CAS estimates are indirect and approximate. They are obtained for a TS by summing up: i) the CASPT2(12,12) energies which correspond either to the CASSCF(12,10) TS, or to the maximum along a CASPT2(12,12) profile (values in italic), and ii) the correction for the enthalpy and free energy coming from the CASSCF (10,8) vibrational analysis carried out on the CASSCF (10,8) critical point.

Formation of the diradicals: Two sp^2-carbon atoms can undergo $^1O_2$ attack, thus yielding different diradical intermediates (**2a** and **b**, Scheme 4). The ene product can originate only from the **2a** attack on the unsubstituted carbon (for this reason **2b** is studied only at the DFT(B3LYP) level), but both can give way to the [π2+π2] cycloaddition. Moreover, although not all the conformational minima of the peroxyl diradical have the terminal oxygen atom and the methyl group

Table 2. DFT relative energies, enthalpies, and free energies (at 298 K).[a]

Structure	Functional	B3LYP			MPW1K			
		ΔE[b]	ΔH	ΔG	ΔE[b]	ΔH	ΔG	ΔE[d]
propene + $^1\Delta_g$ O_2	**1**	0.0	0.0	0.0	0.0	0.0	0.0	0.0
diradical formation	**TS1–2a**	14.2	13.8	23.2	17.5	17.0	26.1	18.0[e]
peroxyl diradical	**2a**	5.7	6.5	16.3	0.8	1.7	11.2	1.2[e]
diradical to hydroperoxide	**TS1–3**	6.7	5.9	17.7	4.5	3.2	15.2	4.8
hydroperoxide	**3**	−31.8	−29.5	−19.1	−35.6	−32.8	−22.8	−35.9
diradical to peroxirane	**TS3–4**	–	–	–	15.2	15.6	27.7	14.8
peroxirane	**4**	18.1[c]	19.9[c]	30.9[c]	12.6	14.6	25.7	12.0
hydrogen abstraction	**TS1–5**	23.9	20.5	28.6	27.9	24.4	32.2	29.0
HOO + allyl radicals	**5**	18.4	16.7	14.4	15.4	13.5	11.3	16.2
diradical to dioxetane	**TS2a–6**	15.2	15.2	25.5	10.8	11.0	21.5	11.0
dioxetane	**6**	−26.8	−24.0	−12.8	−34.4	−31.3	−20.0	−35.7

[a] In kcal mol^{-1}. [b] Energy determined by the method proposed by Yamaguchi (see Methods section). [c] These data are relevant to the *trans* methylperoxirane. [d] ΔE[MPW1K/6–311G(3df,2p)//MPW1K/6–311G(d,p)]. [e] ΔE[MPW1K/aug-cc-pVTZ//MPW1K/6–311G(d,p)] values for **TS1-2a** and **2a** are 18.5 and 1.9 kcal mol^{-1}, respectively.

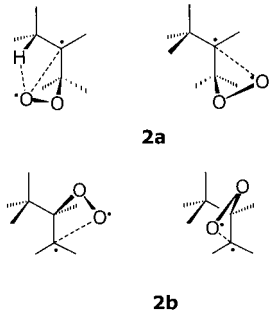

2a **2b**

Scheme 4. Diradical intermediates yielded by the attack of $^1O_2$.

in a favorable mutual orientation for the hydrogen-transfer and the related C=C double bond formation, some of them permit the [π2+π2] cycloaddition (Scheme 4).

The attack which gives **2a** corresponds to a rather high barrier ($\Delta E^{\ddagger}_{MPW1K} = 12.3$, $\Delta E^{\ddagger}_{B3LYP} = 14.2$, and $\Delta E^{\ddagger}_{CASPT2} = 15.7$ kcal mol^{-1}). The diradical **2a** is kinetically stable with respect to back-dissociation through the same TS, with a significant energy barrier, whose height is 11.5 (MPW1K), 8.4 (B3LYP), or 8.6 kcal mol^{-1} (CASPT2). The mode of attack at the methyl-substituted carbon atom to give intermediate **2b** presents a slightly higher barrier ($\Delta E^{\ddagger} = 15.7$ kJ mol^{-1} at the DFT(B3LYP) level). Also, the diradical **2b** is stable with respect to back-dissociation, with a barrier of 4.2 kcal mol^{-1}. Diradical **2b** is higher in energy than **2a** by 5.8 kcal mol^{-1}. Both these minima will be reconsidered when discussing the [π2+π2] pathway and its possible competition with the ene reaction.

Hydroperoxide formation from the diradical 2a: The allyl hydroperoxide product is located at approximately −36.4 (MPW1K), −37.5 (B3LYP), or −40.5 kcal mol^{-1} (CASPT2) below the diradical intermediate **2a**. Figure 1 displays the

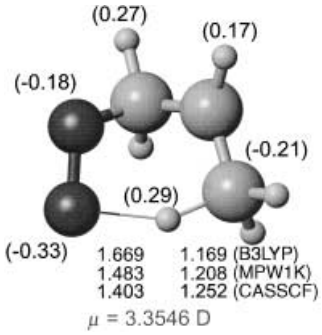

Figure 1. Transition structure **TS 2a–3** for the transformation of the peroxyl diradical **2a** to the product hydroperoxide **3**. The reported interatomic distances are in Ångströms and were calculated at the DFT(B3LYP)/6–311G(d,p), DFT(MPW1K)/6–311G(d,p), CASSCF/6–311G(d,p) levels. The dipole moment was calculated at the DFT(B3LYP) level, the NAO group charges are given in parentheses.

transition structure **TS 2a–3**, relevant to the hydrogen-transfer step that yields the product. This very exoergic step is described as rather easy at the DFT(MPW1K) level (3.8 kcal mol^{-1}), and more so at the DFT(B3LYP) level (1.0 kcal mol^{-1}). The CASPT2/CASSCF single-point computation for **TS 2a–3** even provides a zero energy difference. Given that the actual position of the TS on the CASPT2 surface is unknown,[53] and that our previous experience has shown non-negligible shifts with respect to the CASSCF geometry, an approximate energy profile was built by simply carrying out a linear interpolation of the geometrical parameters at the CASSCF level, given that those of **2a** and **TS 2a–3** are rather close (see the Supporting Information, file energies.xls). This was followed by a series of CASPT2 single-point calculations. The energy profile defines the CASPT2 estimate as 0.6 kcal mol^{-1}, close to the B3LYP value. If this path is compared to that determined at the CASSCF level, its highest-energy point is closer to the diradical minimum **2a**, and suggests an earlier CASPT2 TS.

The pathway to peroxirane: If the spatial relationship between the exocyclic oxygen atom and the methyl group is considered, two isomeric structures of the methyl peroxirane **4** can be drawn, one in which the two groups are approximately *syn* (*cis*-**4**) and one in which they are approximately *anti* (*trans*-**4**). Both structures are stable at the DFT(MPW1K), and are located 11.9 and 11.8 kcal mol^{-1} above the diradical **2a**, respectively. By contrast, *cis*-**4** cannot be optimized at the DFT(B3LYP) level, because the hydrogen transfer typical of the ene reaction is exceedingly easy, and the hydroperoxide product is the only outcome of any optimization attempt. Only the *trans*-**4** isomer can be optimized, which is located 12.4 kcal mol^{-1} above the diradical. An interconversion TS, in which the terminal oxygen atom lies approximately on the three-ring plane (Scheme 5), connects the two stable structures at the DFT(MPW1K). The relevant first-order saddle point corresponds to a barrier (in the *trans* to *cis* direction) of 25 kcal mol^{-1} (Table 2).

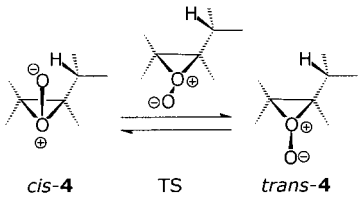

Scheme 5. The interconversion of *cis*-**4** and *trans*-**4**.

A similar TS is found at the DFT(B3LYP) level, and its energy is again 25 kcal mol^{-1} above that of *trans*-**4**. Of course, the saddle point connects in this case *trans*-**4** to the product. Thus, the process is rather high in energy and unlikely, and *trans*-**4** turns out to be uninteresting if the ene process is considered. At the CASSCF level both the *cis*-**4** and *trans*-**4** isomers are found, and are described as stable with respect to both back-dissociation and conversion to the diradical. The estimate of the energy at the CASPT2 level for *cis*-**4** places it 12.4 kcal mol^{-1} above the diradical.

The *direct* formation of *cis* methyl peroxirane from propene and singlet oxygen is not possible. In fact, the saddle point representative of a mode of approach in which the dioxygen and propene moieties combine by taking on a peroxirane-like nuclear configuration (Scheme 6, dashed arrow), is a second-

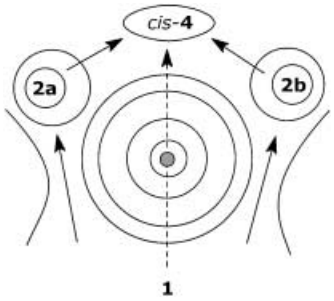

Scheme 6. The second-order saddle point representing the mode of approach of dioxygen and propene.

order saddle point (two imaginary vibrational frequencies), not a transition structure, at the CASSCF level (gray dot).[54] Thus, the relevant structure is not of direct chemical interest, and the peroxirane minimum is attainable by the reacting system only by passing through the diradical intermediates (Scheme 6, arrows). This is consistent with what was found in a previous study.[37]

The role of peroxirane: Although the DFT(B3LYP) computations question the existence of the *cis* methyl peroxirane energy minimum, in contrast with the DFT(MPW1K) results, both calculations locate a perepoxidic structure approximately 12 kcal mol^{-1} above the diradical, just as the multiconfigurational calculations do. This of course casts some doubt on the role of a perepoxidic structure in the ene reaction. Therefore, it was decided to determine the features of the CASPT2 hypersurface in greater detail by a rather large series of single-point energy calculations. The zone of the energy surface that includes the diradical **2a** and the *cis* peroxirane **4**, and connects them with the dominium of the product allyl hydroperoxide **3**, was explored at the CASPT2(12,12)// CASSCF(12,10) level. This part of the study is articulated as follows. The "valley" that connects the CASSCF minima **2a** and *cis*-**4** was delineated by a series of constrained geometry optimizations. In each of these, the subspace of the geometrical parameters is defined by holding the angle defined by the atoms CCO fixed to one value between the extremes of $<\mathrm{CCO} = 61^\circ$ (pertaining to *cis*-**4**) and $<\mathrm{CCO} = 105^\circ$ (pertaining to **2a**) and optimizing the remaining parameters. In a parallel fashion, starting from the **TS2a–3** ($<\mathrm{CCO} = 98^\circ$) a "ridge" was determined that extends in the direction of peroxirane. The scan was carried out by a series of constrained hydrogen-transfer first-order saddle point searches. Again, the CCO angle was the variable chosen to scan the ridge, within the geometrical subspace just defined. Along the ridge, the MCSCF geometries determined at various values of the CCO angle share a fundamental feature with the critical point **TS2a–3**: the methyl C–H bond is rather short, and the corresponding O–H bond rather long. In the final points of each optimization the first Hessian eigenvector resembles that of the transition structure **TS2a–3**. Finally, the direction connecting some selected points of the valley to the corresponding points along the ridge (i.e. in correspondence with the same CCO value) was probed, by simply performing linear interpolations of the geometrical parameters. This overall setting is apparent in Figure 2, where the displayed

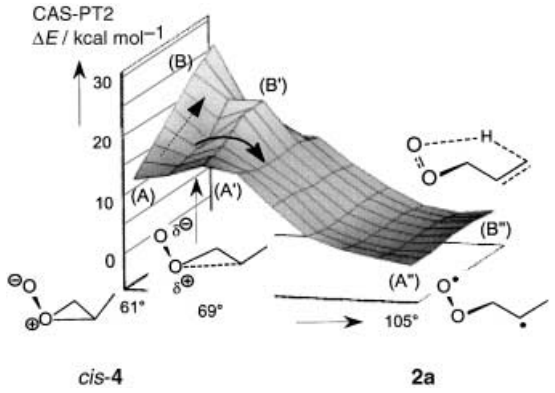

Figure 2. Three-dimensional map built by a series of single-point CASPT2(12,12) calculations, carried out on CASSCF(12,10) geometries. The surface includes the diradical **2a** (zero of the energy) and the *cis*-peroxirane **4** (foreground), and connects them with the dominium of the allyl hydroperoxide **3** (background).

surface is a representation of the CASPT2 energies collected in correspondence of all CAS–MCSCF geometries. The part of the surface closer to the reader is the valley, marked (A), (A′) and (A″) in Figure 2, that joins the two minima, whereas the more remote part includes the ridge, marked (B), (B′), and (B″), beyond which the surface goes down to the hydroperoxide minimum. Along the section (A)–(A′)–(A"), the *cis* peroxirane is found on the left, 12.4 kcal mol^{-1} above the diradical, which is on the right. The valley and the ridge are the common qualitative features shared by the CASSCF and CASPT2 surfaces.

However, the CASPT2 energy hypersurface is shifted with respect to the CASSCF: this results in an earlier position of **TS2a–3** with respect to the diradical as already seen previously, and, in much the same way, of the whole ridge. Thus, the CASPT2 points corresponding to the MCSCF ridge (farthest left-to-right line in the surface of Figure 2) lie beyond the CASPT2 ridge (B). In addition to the fact that *cis*-**4** is at higher energy than **2a**, two important points can be gathered from the three-dimensional plot. 1) The transformation **2a–4** is possible ($\Delta E^{\ddagger}_{\mathrm{CASPT2}} \approx 15.7$ kcal mol^{-1}), but the back-transformation is much easier ($\Delta E^{\ddagger}_{\mathrm{CASPT2}} \approx 2.9$ kcal mol^{-1}). 2) Even more importantly, and apparent upon inspection of Figure 2, the **4–2a** back-transformation would be significantly easier for the system than ascending the leftmost valley (dashed arrow) from *cis*-**4** toward the hydroperoxide **3** ($\Delta E^{\ddagger}_{\mathrm{CASPT2}} \approx 14.0$ kcal mol^{-1}). The entire valley is not well protected with respect to the wide lower-energy dominium of the diradical minimum, which lies on the right. As the system ascends the valley, overcoming the low ridge that separates it from the broad basin on the right becomes easier and easier: the height of the (A′)–(B′) ridge with respect to the ascending valley goes down from approximately 2.9 kcal mol^{-1} in correspondence of the (A)–(A′)–(A″) valley, that is of **TS2a–4** (vertical arrow), to less than 0.5 kcal mol^{-1} in correspondence of the (B)–(B′)–(B″) ridge: overcoming this low ridge that separates the uphill valley from the broad basin on the right (curved arrow) should be easier than climbing the valley. Thus, no liable reaction pathway is associated with the *cis* peroxirane **4**. The descent into the

product domain has to take place through the diradical intermediate **2a** and **TS 2a–3**.

Concerted hydroperoxide formation from $^1O_2$ and propene: Another important point would be to ascertain whether a concerted pathway is open to this system, in competition with the two-step diradical pathway. This would imply the formation of one oxygen–carbon bond as well as a methyl-hydrogen transfer to the other oxygen (O′) taking place in the same kinetic step. The two-dimensional map displayed in Figure 3 attempts to give an overall view of the relationship

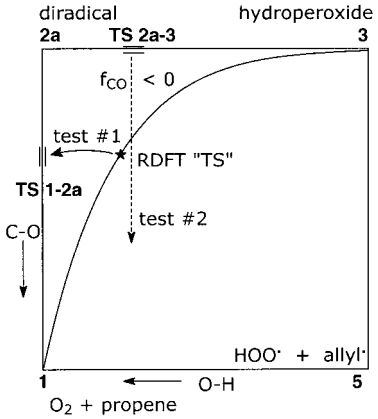

Figure 3. Two nonconcerted pathways (**1**–**2a**–**3** and **1**–**5**–**3**) connect the reactants **1** to the allyl hydroperoxide **3**. The postulated concerted pathway (approximately diagonal curve) is found in correspondence of a restricted DFT calculation. This defines a RDFT "TS", which does not exist as the following tests show. Test #1: the stability of the DFT wavefunction at the "TS" with respect to orbital rotations is tested and found to be unstable; the orbitals are relaxed along the direction of instability, until a stable solution is found; then a TS search is run and converges onto **TS 1–2a**. Finally, a CASSCF TS search starting from the geometry of the RDFT "TS" gives **TS 1–2a** again. Test #2: constrained hydrogen-transfer "TS" CASSCF optimizations, which generate points along a ridge for fixed C–O values (1.7–2.9 Å): the force along C–O is always negative.

between the two pathways discussed in this subsection and in that dealing with dioxetane formation. In Figure 3, the putative concerted transformation of the two reactants **1** directly to the hydroperoxide **3** would lie on the approximately diagonal curve. In a recent paper on the ene reaction of singlet oxygen with cyclohexene, a concerted pathway was found at the restricted DFT (RDFT) level.[55] Indeed, when searching for a concerted transition structure at the UDFT(-B3LYP) level of theory, the unrestricted self-consistent procedure converged right from the beginning on a restricted wavefunction, and a TS was found at this point (star in Figure 3). This RDFT TS (vibrational frequencies calculation in the Supporting Information) has a rather usual C–O length (1.930 Å), but can be classified as rather early as concerns the hydrogen transfer. In fact, a large O′–H length (1.809 Å) corresponds to a C–H bond that is moderately stretched (1.137 Å). The soundness of this result has been carefully scrutinized for our system as follows (test #1: see Figure 3 and the Supporting Information). 1) The TS wavefunction was tested to check its stability with respect to orbital rotations,[56–58] and found to be *unstable*. 2) When the orbitals were relaxed along the instability direction, a new stable solution was found. The new UDFT solution coincides with that obtainable by the orbital switching procedure (see the Methods section), that had already been used when dealing with diradicals, diradicaloid structures,[38] homolysis and radical coupling.[59] This wavefunction now has acceptable spin densities and a qualitatively proper spin polarization that allows to it to correlate back to the reactants, upon re-dissociation of the two moieties, in a correct way. In particular, the system evolves toward an adequate description of $^1\Delta_g$ O_2. 3) If this stable wavefunction is used to search for the TS over again, and the analytic Hessian is computed before starting, the TS for the formation of the diradical from the two reactants (**TS 1–2a**) is found instead: no trace of the restricted-DFT transition structure is present on the unrestricted surface.

Then, given that a multideterminantal wavefunction should more easily accommodate the spin recoupling patterns associated with a concerted transition structure, this TS was again searched for at the CASSCF level, starting from the geometry provided by the restricted DFT calculations. These searches were unsuccessful, since the diradical formation TS was found again. A further probing of the reaction surface was performed at the CASSCF level (Figure 3: test #2). By taking the diradical to hydroperoxide **TS 2a–3** as a starting point, a series of constrained hydrogen-transfer first-order saddle point searches was carried out at fixed C–O lengths. If the dominium of a concerted TS were intersected, the only nonzero residual force, that along the C–O, should at some point in the proximity of point marked with the star in Figure 3 change its sign from negative to positive. These optimizations went along a ridge, spanning a 1.7 to 2.9 Å C–O length range. The force along the C–O was negative at all times, thus providing an indication that a concerted transition structure is absent on the CASSCF hypersurface.

Hydroperoxide formation by means of hydrogen-abstraction/radical coupling: Another conceivable two-step reaction pathway begins with a hydrogen transfer from propene to $^1O_2$. It generates the radical pair allyl and hydroperoxyl **5**. This step requires 27.9 (MPW1K), 23.9 (B3LYP), or 33.6 kcal mol^{-1} (CASPT2). The allyl and hydroperoxyl radicals are 15.4 (MPW1K), 18.4 (B3LYP), or 18.7 kcal mol^{-1} (CASPT2) above the two reactants. They can then very easily couple, to give the final hydroperoxide product. However, at all theory levels, the TS is significantly higher than the diradical formation TS, which requires, as seen, 12.3 (MPW1K), 14.2 (B3LYP), or 15.7 kcal mol^{-1} (CASPT2).

Consequently, this hydrogen-abstraction/radical recombination pathway cannot compete efficiently. The overall energy profiles for the transformations examined so far are displayed in Figure 4. Bold numerals used in the tables are used also in the energy profiles to mark the critical points consistently. Thus, on the left in Figure 4, the diradical formation pathway is recognizable as marked by: **1**, **TS 1–2a**, **2a**, and the diradical transformation to the hydroperoxide as: **2a**, **TS 2a–3**, **3**. Finally, the last two-step pathway just presented as **1**, **TS 1–5**, **5**.

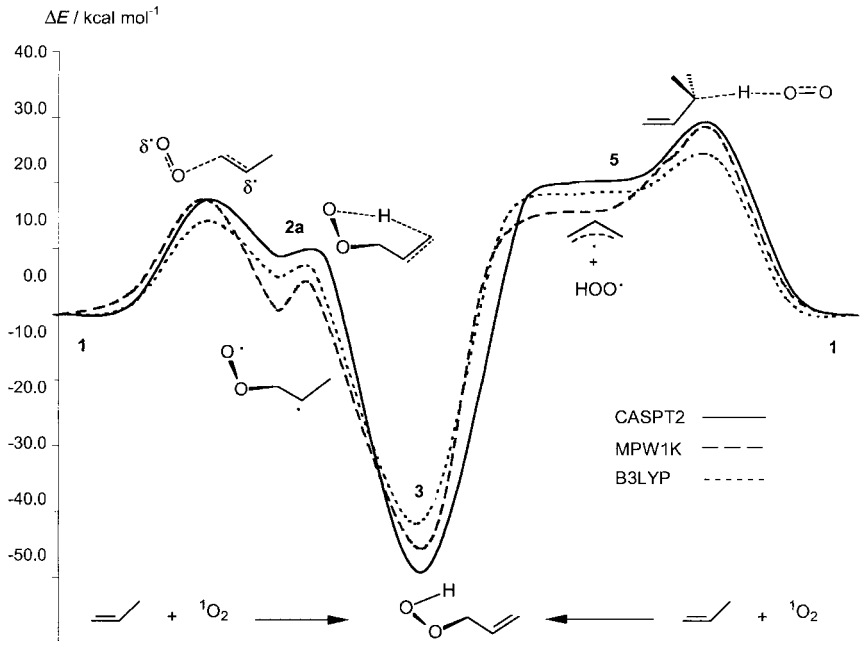

Figure 4. CASPT2 and DFT (MPW1K and B3LYP) energy profiles for two nonconcerted pathways in the gas-phase ene reaction of singlet dioxygen and propene.

Dioxetane formation pathway from the diradical: The [π2+π2] cycloaddition, which in this case produces the methyl dioxetane **6**, is rather often found to compete with the ene pathway. The outcome of the competition between the two reactions is altered, in general, by the nature of the alkene and solvent effects. Several experiments (see for instance references [18–20]) indicate that the [π2 + π2] cycloaddition should have a more polar TS than the ene pathway, because as the solvent becomes more polar, the cycloaddition becomes more competitive.

For our system, we find that the energy of methyl dioxetane **6** is −35.2 (MPW1K), −32.5 (B3LYP), or −37.0 kcal mol^{-1} (CASPT2) with respect to the diradical intermediate **2a**. Thus, as was the case for the allyl hydroperoxide, the reaction step is quite exoergic. However, the energy barriers for the [π2+π2] reaction that originates from the diradical **2a** (10.1 (MPW1K), 9.5 (B3LYP), 10.7 kcal mol^{-1} (CASPT2)) are significantly higher than those for the ene reaction at all levels (the transition structure **TS 2a–6** for diradical closure to dioxetane is shown in Figure 5).

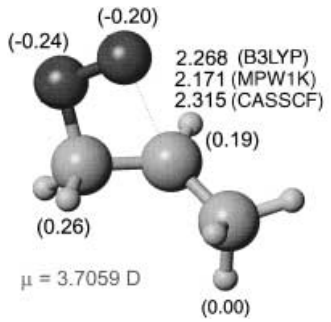

Figure 5. Transition structure **TS 2a–6** for the formation of methyl dioxetane **6**. The reported interatomic distances are in Ångströms and were calculated at the DFT(B3LYP)/6–311G(d,p), DFT(MPW1K)/6–311G(d,p), and CASSCF/6–311G(d,p) levels. The dipole moment was calculated at the DFT(B3LYP) level, the NAO group charges are given in in parentheses.

The difference ($\Delta E_{2+2} - \Delta E_{ene}$) is 6.3 at the MPW1K, 8.5 at the B3LYP, and 10.2 kcal mol^{-1} at the CASPT2, thus in favor of the ene pathway (Figure 6). Yet, in contrast with a single ene pathway, which has its origin in one conformation of **2a**, the dioxetane can form through different channels, which originate not only from a second conformation of **2a** (see Scheme 4), but also from those of **2b**. Thus, the ΔG values reported in Tables 1 and 2 should allow one to estimate the branching ratio for the ene and [2+2] pathways. Due to the rather indirect way by which the CAS estimates of G have been obtained, we prefer to make use of the DFT values to approximately determine k_{ene}/k_{2+2}. Kinetic equations were derived within the steady-state approximation, applied to the diradical intermediates **2a** and **2b**, each in two conformations, and can be found in the Supporting Information along with other details. The interconversion of the conformations has been taken into account for both diradicals, as well as the fact that **2a** and **2b** can interconvert only by re-dissociating. The result, at the DFT(B3LYP) level, is a factor of almost 3×10^3 in favor of the ene channel.

We have already commented that the distinction between a zwitterion and a diradical must not be held as too rigid, because a carbon–oxygen diradical has some zwitterionic character (e.g. $\mu = 2.853$ D, at the DFT(B3LYP) level).[40] A sharper zwitterionic character may be related to excited electronic states of the open-chain molecule, but polar diradicals are representative of pathways involving open-chain intermediates. The dipole moments of the two transition structures are different, but the difference is not very large. For instance, at the DFT(B3LYP) level, the diradical to hydroperoxide **TS 2a–3** has a $\mu^{\pm}$ value of 3.355 D, while for the diradical to dioxetane **TS 2a–6** the $\mu^{\pm}$ value is 3.706 D. This difference is further illustrated by the NAO charges reported in Figure 1 and Figure 5. At this point, it is interesting to assess to what degree a polar solvent might be able to stabilize the diradical intermediate and the two transition structures, on the basis of their intrinsic polarity.

Solvent simulation is limited in this paper to "solvating" the gas-phase system with a polarizable continuum. This is done by the Onsager–Kirkwood and Tomasi methods (solvent: acetonitrile). The former provides only a slight stabilization of the cycloaddition TS relative to the ene TS (ca. 1.1 kcal mol^{-1}). On the other hand, DFT(B3LYP)/PCM single-point energy calculations and subsequent re-optimization of the

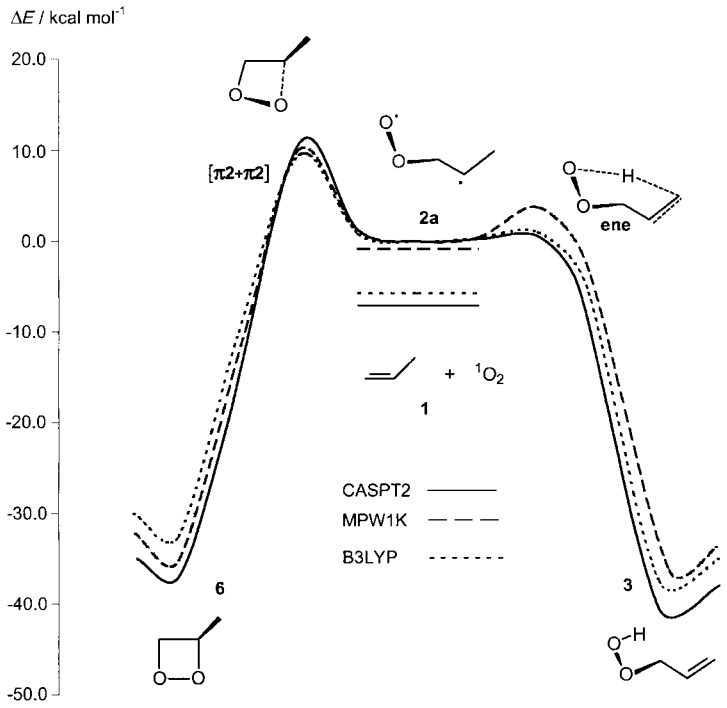

Figure 6. CASPT2 and DFT (MPW1K and B3LYP) energy profiles for the gas-phase ene and [π2+π2] cycloaddition reaction of singlet dioxygen and propene. The reactants are represented by three horizontal lines.

geometries within the DFT/PCM scheme provide a rather disappointing result in that this small effect disappears. The DFT/PCM results do not alter at all the picture presented for the gas-phase reaction, neither qualitatively (optimization of the critical points), nor quantitatively (energy differences). Additional data on these tests are provided in the Supporting Information. More significant effects could be expected if protic solvents (e.g. methanol) were considered, but this aspect of the study requires a more demanding investigation, because the approach would consist in building a "supermolecule" cluster, by explicitly associating the reactants and one or more solvent molecules, followed, for instance, by the PCM estimate of the solvent effects. This extension is reserved for a follow-up study of the ene reaction in protic solvents, which is currently underway.

Thus, the final indication is that the only practicable pathway for this system is the ene, via the diradical intermediate. The rate-determining step along this pathway is diradical formation. The enthalpy data of Table 1 and Table 2 can be compared with the data obtained from an early gas-phase kinetic study by Ashford and Ogryzlo,[60] in which the Arrhenius parameters for a series of bi-, tri-, and tetrasubstituted alkenes were determined. The only outcome of the photo-oxidations studied was hydroperoxide formation (as apparent from Table V in reference [60]). Our $\Delta H + RT$ values for propene are in fair agreement with the qualitative trend shown by the experimental E_a values as a function of the degree of substitution. Consistently with the non-negligible polarity exhibited by the transition structure for diradical formation ($\mu^{\neq} = 2.552$ D for **TS1–2a**), our DFT(B3LYP)/PCM solvent simulations reduce the rather high energy barrier for diradical formation computed in the gas phase (14.2 kcal mol^{-1}) by an extent that depends on the solvent polarity: the barrier goes down to 12.2 kcal mol^{-1} for $CHCl_3$, while for acetonitrile a further drop to 11.3 kcal mol^{-1} is estimated. Our computations indicate that the entropy change has a significant effect on the gas-phase free energy barrier: $\Delta S^{\neq} = -30$ to -34 cal mol^{-1} K^{-1}, depending on the theory level, as expected for the formation of an adduct. The important role of entropy was stressed in reference [31].

Conclusions

The gas-phase mechanism of both the ene and [π2+π2] reactions in the $O_2 + CH_2 = CH{-}CH_3$ system (**1**) have been investigated. The main result of this study is that a two-step ene pathway passing through a polar diradical intermediate (**2a**) is sharply favored. Diradical formation is described as nonreversible. Another major result is that a peroxirane (**4**) pathway is ruled out, at least as regards this system, by the energetics and by the qualitative features of the hypersurface. Of course, further investigation on more complex systems is advisable before taking this result as applicable in general. A concerted pathway, flanking the nonconcerted diradical pathway, and connecting directly the reagents **1** to the hydroperoxide product **3**, is suggested by a restricted DFT calculation. This possibility is carefully examined and discarded as an artifact of the restricted setting. A second nonconcerted pathway (hydrogen abstraction operated by O_2 on propene, followed by hydroperoxyl and allyl radical coupling to give **3**) is not competitive. Also the [π2+π2] cycloaddition, which stems from the same diradical intermediate, cannot compete in this system with the very easy **2a–3** ene step. The ene channel is preferred by a factor of the order of 10^3. Given that the cycloaddition TS is slightly more polar than the ene, we attempted to simulate the effect of a polar solvent (CH_3CN) by two methods, to assess its effectiveness in tuning the competition more in favor of the cycloaddition. One simulation gave a very small effect in that sense, while the other was basically ineffective.

Acknowledgement

Financial support was provided by the Italian MURST (now MIUR), within the Programma di Ricerca Scientifica di Rilevante Interesse Nazionale "Chimica in Fase Gassosa di Specie Reattive Neutre e Cariche", year 2001.

[1] A. Gilbert, J. Baggott, *Essentials of Molecular Photochemistry*, Blackwell Science, **1995**, Chapter 11.

[2] a) C. S. Foote, E. L. Clennan, "Properties and Reactions of Singlet Dioxygen" in *Active Oxygen in Chemistry* (Eds.: C. S. Foote, J. S. Valentine, A. Greenberg, J. F. Liebman), Blackie Academic and Professional (Chapmann & Hall), **1995**, Chapter 4; b) R. Atkinson, "Reactions of Oxygen Species in the Atmosphere" in *Active Oxygen in Chemistry* (Eds.: C. S. Foote, J. S. Valentine, A. Greenberg, J. F. Liebman), Blackie Academic and Professional (Chapmann & Hall), **1995**, Chapter 7; c) P. Dussault "Reactions of Hydroperoxides and Peroxides", in *Active Oxygen in Chemistry* (Eds.: C. S. Foote, J. S. Valentine, A. Greenberg, J. F. Liebman), Blackie Academic and Professional (Chapmann & Hall), **1995**, Chapter 5, pp. 176, 177; d) B. H. Bielski, D. E. Cabelli, "Superoxide and Hydroxyl Radical Chemistry in Aqueous Solution" in *Active Oxygen in Chemistry*, (Eds.: C. S. Foote, J. S. Valentine, A. Greenberg, J. F. Liebman), Blackie Academic and Professional (Chapmann & Hall), **1995**, Chapter 3; e) see ref. [2a], pp. 107–109, 119, 120, and 132, for some recent studies.

[3] R. P. Wayne, *Chemistry of Atmospheres*, Clarendon Press, Oxford, **1996**, p. 86.

[4] a) B. Plesnicar "Polyoxides" in *Organic Peroxides* (Ed.: W. Ando), Wiley, **1992**, Chapter 10, pp. 489–494; b) K. Yamaguchi, K. Takada, Y. Otsuji, K. Mizuno "Theoretical and General aspects of Organic Peroxides", in *Organic Peroxides* (Ed.: W. Ando), Wiley, **1992**, Chapter 1, pp. 65–68.

[5] a) R. A. Marusak, C. F. Meares "Metal-Complex Catalyzed Cleavage of Biopolymers" in *Active Oxygen in Biochemistry* (Eds.: J. S. Valentine, C. S. Foote, A. Greenberg, J. F. Liebman), Blackie Academic and Professional (Chapmann & Hall), **1995**, Chapter 8; b) B. Halliwell, "The Biological Significance of Oxygen-Derived Species" in *Active Oxygen in Biochemistry* (Eds.: J. S. Valentine, C. S. Foote, A. Greenberg, J. F. Liebman), Blackie Academic and Professional (Chapmann & Hall), **1995**, Chapter 7; c) A. Greenberg, "Exploration of Selected Pathways for Metabolic Oxidative Ring Opening of Benzene Based on Estimates of Molecular Energetics" in *Active Oxygen in Biochemistry* (Eds.: J. S. Valentine, C. S. Foote, A. Greenberg, J. F. Liebman), Blackie Academic and Professional (Chapmann & Hall), **1995**, Chapter 9, pp. 415–419.

[6] a) M. B. Smith, J. March, *March's Advanced Organic Chemistry. Reactions, Mechanisms, and Structure*, 4th ed., Wiley, **2001**, chapter 15, Sections 14–8, 15–20 and 15–49; b) B. K. Carpenter, *Determination of Organic Reaction Mechanisms*, Wiley, **1984**, Chapter 9, Section 4.

[7] C. W. Jefford, *Chem. Soc. Rev.* **1993**, 59–66.

[8] A. A. Frimer, *Chem. Rev.* **1979**, *79*, 359–387.

[9] H. M. R. Hoffmann, *Angew. Chem.* **1969**, *81*, 597–608; *Angew. Chem. Int. Ed. Engl.* **1969**, *8*, 556–577.

[10] G. O. Schenck, H. Eggert, W. Denk, *Liebigs Ann. Chem.* **1953**, *584*, 177–198.

[11] M. Prein, W. Adam, *Angew. Chem.* **1996**, *108*, 519–538; *Angew. Chem. Int. Ed. Engl.* **1996**, *35*, 477–494, and references [7–23] therein.

[12] H. Mori, K. Ikoma, S. Isoe, K. Kitaura, S. Katsumura, *Tetrahedron Lett.* **1996**, *37*, 7771–7774; H. Mori, K. Ikoma, S. Katsumura, *Chem. Commun.* **1997**, 2243–2244; H. Mori, K. Ikoma, S. Isoe, K. Kitaura, S. Katsumura, *J. Org. Chem.* **1998**, *63*, 8704–8718; H. Mori, T. Matsuo, K. Yamashita, S. Katsumura, *Tetrahedron Lett.* **1999**, *40*, 6461–6464.

[13] E. A. Lissi, M. V. Encinas, E. Lemp, M. A. Rubio, *Chem. Rev.* **1993**, *93*, 699–723.

[14] I. Fleming, *Pericyclic Reactions,* Oxford Science Publications, Oxford University Press, **1999**, pp. 84–86.

[15] See for instance: E. L. Clennan, *Tetrahedron* **1991**, *47*, 1343–1382 (Tetrahedron Report no. 285).

[16] A. A. Gorman, I. R. Gould, I. Hamblett, *J. Am. Chem. Soc.* **1982**, *104*, 7098–7104.

[17] K. H. Schulte-Elte, V. Rautenstrauch, *J. Am. Chem. Soc.* **1980**, *102*, 1738–1740; W. Adam, L. H. Catalani, A. Griesbeck, *J. Org. Chem.* **1986**, *51*, 5494–5496; W. Adam, B. Nestler, *J. Am. Chem. Soc.* **1992**, *114*, 6549–6550; W. Adam, B. Nestler, *J. Am. Chem. Soc.* **1993**, *115*, 5041–5049; H.-G. Brünker, W. Adam, *J. Am. Chem. Soc.* **1995**, *117*, 3976–3982; T. Linker, F. Rebien, G. Tóth, *Chem. Commun.* **1996**, 2585–2586; W. Adam, H.-G. Brünker, A. S. Kumar, E.-M. Peters, K. Peters, U. Schneider, H. G. v. Schnering, *J. Am. Chem. Soc.* **1996**, *118*, 1899–1905.

[18] W. Adam, C. R. Saha-Möller, S. B. Schambony, *J. Am. Chem. Soc.* **1999**, *121*, 1834–1838.

[19] G. Vassilikogiannakis, M. Stratakis, M. Orfanopoulos, *J. Org. Chem.* **1998**, *63*, 6390–6393.

[20] A. A. Frimer, P. D. Bartlett, A. F. Boschung, J. G. Jewett, *J. Am. Chem. Soc.* **1977**, *99*, 7977–7986.

[21] a) G. Vassilikogiannakis, M. Stratakis, M. Orfanopoulos, C. S. Foote, *J. Org. Chem.* **1999**, *64*, 4130–4139; b) M. Stratakis, M. Orfanopoulos, C. S. Foote, *J. Org. Chem.* **1998**, *63*, 1315–1318; c) M. Stratakis, M. Orfanopoulos, C. S. Foote, *Tetrahedron Lett.* **1996**, *37*, 7159–7162; d) M. Stratakis, M. Orfanopoulos, J. S. Chen, C. S. Foote, *Tetrahedron Lett.* **1996**, *37*, 4105–4108; e) Y. Elemes, C. S. Foote, *J. Am. Chem. Soc.* **1992**, *114*, 6044–6050; f) M. Orfanopoulos, I. Smonou, C. S. Foote, *J. Am. Chem. Soc.* **1990**, *112*, 3607–3614; g) M. Orfanopoulos, C. S. Foote, *J. Am. Chem. Soc.* **1988**, *110*, 6583–6584; h) K. Gollnick, H. Hartmann, H. Paur in *Oxygen and Oxy-radicals in Chemistry and Biology* (Eds.: E. L. Powers, M. A. J. Rodgers), Academic Press, New York, **1981**, pp. 379–395; i) M. B. Grdina, M. Orfanopoulos, L. M. Stephenson, *J. Am. Chem. Soc.* **1979**, *101*, 3111–3112; j) L. M. Stephenson, D. E. Mc Clure, P. K. Sysak, *J. Am. Chem. Soc.* **1973**, *95*, 7888–7889.

[22] K. R. Kopecky, J. H. van de Sande, *Can. J. Chem.* **1972**, *50*, 4034–4049.

[23] A. G. Griesbeck, M. Fiege, M. S.Gudipati, R. Wagner, *Eur. J. Org. Chem.* **1998**, 2833–2838.

[24] J.-M. Aubry, B. Mandard-Cazin, M. Rougee, R. V. Bensasson, *J. Am. Chem. Soc.* **1995**, *117*, 9159–9164.

[25] R. C. Kanner, C. S. Foote, *J. Am. Chem. Soc.* **1992**, *114*, 682–688.

[26] E. L. Clennan, R. P. L'Esperance, *J. Am. Chem. Soc.* **1985**, *107*, 5178–5182; E. L. Clennan, R. P. L'Esperance, *J. Org. Chem.* **1985**, *50*, 5424–5426; E. L. Clennan, K. K. Lewis, *J. Am. Chem. Soc.* **1987**, *109*, 2475–2478; E. L. Clennan, K. Nagraba, *J. Am. Chem. Soc.* **1988**, *110*, 4312–4318.

[27] K. E. O'Shea, C. S. Foote, *J. Am. Chem. Soc.* **1988**, *110*, 7167–7170.

[28] T. H. W. Poon, K. Pringle, C. S. Foote, *J. Am. Chem. Soc.* **1995**, *117*, 7611–7618.

[29] A. Greer, G. Vassilikogiannakis, K.-C. Lee, T. S. Koffas, K. Nahm, C. S. Foote, *J. Org. Chem.* **2000**, *65*, 6876–6878.

[30] A. P. Schaap, G. R. Faler, *J. Am. Chem. Soc.* **1973**, *95*, 3381–3382; A. P. Schaap, K. A. Zaklika, "1,2 Cycloadditions Reactions of Singlet Oxygen" in *Singlet Oxygen* (Eds.: H. H. Wasserman, R. W. Murray), Academic Press: New York, **1979**, chapter 6; K. A. Zaklika, B. Kaskar, A. P. Schaap, *J. Am. Chem. Soc.* **1980**, *102*, 386–389; A. P. Schaap, S. G. Recher, G. R. Faler, S. R. Villasenor, *J. Am. Chem. Soc.* **1983**, *105*, 1691–1693.

[31] J. R. Hurst, S. L. Wilson, G. B. Schuster, *Tetrahedron* **1985**, *41*, 2191–2197; J. R. Hurst, G. B. Schuster, *J. Am. Chem. Soc.* **1982**, *104*, 6854–6856.

[32] S. Inagaki, S. Yamabe, H. Fujimoto, K. Fukui, *Bull. Chem. Soc. Jpn.* **1972**, *45*, 3510–3514; S. Inagaki, K. Fukui *J. Am. Chem. Soc.* **1975**, *97*, 7480–7484; M. J. S. Dewar, *Chem. Br.* **1975**, *11*, 97–106; M. J. S. Dewar, W. Thiel, *J. Am. Chem. Soc.* **1975**, *97*, 3978–3986; M. J. S. Dewar, A. C. Griffin, W. Thiel, I. J. Turchi, *J. Am. Chem. Soc.* **1975**, *97*, 4439–4440.

[33] L. B. Harding, W. A. Goddard, III, *J. Am. Chem. Soc.* **1977**, *99*, 4520–4523; L. B. Harding, W. A. Goddard, III *Tetrahedron Lett.* **1978**, *8*, 747–750; L. B. Harding, W. A. Goddard, III, *J. Am. Chem. Soc.* **1980**, *102*, 439–449.

[34] K. Yamaguchi, S. Yabushita, T. Fueno, K. N. Houk, *J. Am. Chem. Soc.* **1981**, *103*, 5043–5046.

[35] M. Hotokka, B. Roos, P. J. Siegbahn, *J. Am. Chem. Soc.* **1983**, *105*, 5263–5269.

[36] G. Tonachini, H. B. Schlegel, F. Bernardi, M. A. Robb, *J. Mol. Struct. Theochem.* **1986**, *138*, 221–227; G. Tonachini, H. B. Schlegel, F. Bernardi, M. A. Robb, *J. Am. Chem. Soc.* **1990**, *112*, 483–491.

[37] A. Maranzana, *Tesi di Laurea*, Università di Torino, II Facoltà di Scienze, Sede di Alessandria December, **1997**; A. Maranzana, G. Ghigo, G. Tonachini, *J. Am. Chem. Soc.* **2000**, *122*, 1414–1423.

[38] A. Liwo, D. Dyl, D. Jeziorek, M. Nowacka, T. Ossowski, W. Woznicki, *J. Comput. Chem.* **1997**, *18*, 1668–1681.

[39] M. Bobrowski, A. Liwo, S. Oüdziej, D. Jeziorek, T. Ossowski, *J. Am. Chem. Soc.* **2000**, *122*, 8112 – 8119.

[40] L. Salem, C. Rowland, *Angew. Chem.* **1972**, *84*, 86 – 105; *Angew. Chem. Int. Ed. Engl.* **1972**, *11*, 92 – 111; K. Jug, A. Poredda, *Chem. Phys. Lett.* **1990**, *171*, 394 – 399; K. Jug, C. Kölle, *J. Phys. Chem. B* **1998**, *102*, 6605 – 6611; K. Jug, *Tetrahedron Lett.* **1985**, *26*, 1437 – 1440; J. Michl, V. BonaŠi′-Kouteckyý, *Electronic Aspects of Organic Photochemistry*, Wiley, **1990**, chapter 4, Section 4; J. Michl, V. BonaŠi′-Kouteckyý, *Tetrahedron* **1988**, *44*, 7559 – 7585; V. BonaŠi′-Kouteckyý, J. Kouteckyý, J. Michl, *Angew. Chem.* **1987**, *99*, 219 – 238; *Angew. Chem. Int. Ed. Engl.* **1987**, *26*, 170 – 189.

[41] a) W. J. Hehre, R. Ditchfield, J. A. Pople, *J. Chem. Phys.* **1972**, *56*, 2257 – 2261; P. C. Hariharan, J. A. Pople, *Theor. Chim. Acta* **1973**, *28*, 213 – 222; M. J. Frisch, J. A. Pople, J. S. Binkley, *J. Chem. Phys.* **1984**, *80*, 3265 – 3269; b) T. H. Dunning, *J. Chem. Phys.* **1989**, *90*, 1007 – 1023.

[42] H. B. Schlegel, in *Computational Theoretical Organic Chemistry* (Eds.: I. G. Csizsmadia, and R. Daudel), Reidel, Dordrecht, The Netherlands, **1981**, p. 129 – 159; H. B. Schlegel, *J. Chem. Phys.* **1982**, 77 3676 – 3681; H. B. Schlegel, J. S. Binkley, J. A. Pople, *J. Chem. Phys.* **1984**, *80*, 1976 – 1981; H. B. Schlegel, *J. Comput. Chem.* **1982**, *3*, 214 – 218.

[43] B. O. Roos , P. R. Taylor, P. E. M. Siegbahn, *Chem. Phys.* **1980**, *48*, 157; see also, for a discussion of the method: B. Roos, "The Complete Active Space Self-Consistent Field Method and its Applications in Electronic Structure Calculations", in: *Ab Initio Methods in Quantum Chemistry-II* (Ed: K. P. Lawley), Wiley, **1987**. The implementation of this kind of approach in the Gaussian program system (ref. [49]) is documented in: D. Hegarty, M. A. Robb, *Mol. Phys.* **1979**, *38*, 1795 – 1812; R. H. A. Eade, M. A. Robb, *Chem. Phys. Lett.* **1981**, *83*, 362 – 368.

[44] K. Andersson, P.-Å. Malmqvist, B. O. Roos, A. J. Sadlej, K. Wolinski, *J. Phys. Chem*. **1990**, *94*, 5483 – 5488; K. Andersson, P.-Å. Malmqvist, B. O. Roos, *J. Chem*. *Phys.* **1992**, *96*, 1218 – 1226; B. O. Roos, K. Andersson, M. P. Fülscher, P.-Å. Malmqvist, L. Serrano-Andres, K. Pierloot, M. Mercham, *Adv. Chem. Phys.* **1996**, 93, 219 – 331.

[45] J. A. Pople, P. M. W. Gill, B. G. Johnson, *Chem. Phys. Lett.* **1992**, *199*, 557 – 560.

[46] a) R. G. Parr, W. Yang, *Density Functional Theory of Atoms and Molecules*, Oxford University Press. New York, **1989**, chapter 3; b) W. Koch, M. C. Holthausen, *A Chemist's Guide to Density Functional Theory*, Wiley VCH, **2000**; c) B3LYP functional: A. D. Becke, *Phys. Rev. A* **1988**, *38*, 3098 – 3100; A. D. Becke, *ACS Symp. Ser.* **1989**, *394*, 165; A. D. Becke, *J. Chem. Phys.* **1993**, *98*, 5648 – 5652; C. Lee, W. Yang, R. G. Parr, *Phys. Rev. B* **1988**, *37*, 785 – 789; d) MPW1K functional: B. J. Lynch, P. L. Fast, M. Harris, D. G. Truhlar, *J. Phys. Chem. A* **2000**, *104*, 4811 – 4815, and references therein; B. J. Lynch, D. G. Truhlar, *J. Phys. Chem. A* **2001**, *105*, 2936 – 2941; B. J. Lynch, D. G. Truhlar, *J. Phys. Chem. A* **2002**, *106,* 842 – 846; e) F. Jensen, *Introduction to Computational Chemistry*, Wiley VCH, **1999**, chapter 5 and 6.

[47] a) S. Yamanaka, T. Kawakami, K. Nagao, K. Yamaguchi, *Chem. Phys. Lett.* **1994**, *231*, 25 – 33; K. Yamaguchi, F. Jensen, A. Dorigo, K. N. Houk, *Chem. Phys. Lett.* **1988**, *149*, 537 – 542. b) A couple of calculations on $^1O_2$ and $^3O_2$ can exemplify the procedure. The reference experimental value for the singlet-triplet energy gap is 22.5 kcal mol^{-1}. The original DFT(UB3LYP) calculation would give an energy difference of 39.3 kcal mol^{-1}, in correspondence of a zero $\langle S^2\rangle$ value for $^1O_2$. Enforcing spin contamination in the $^1O_2$ computation by the orbital mixing procedure provides an $\langle S^2\rangle$ value of 1.0035, intermediate between the values of singlet and triplet multiplicities. The singlet – triplet energy gap is now reduced accordingly to 10.4 kcal mol^{-1}. Finally, the projection procedure corrects the energy and produces a singlet – triplet gap of 20.9 kcal mol^{-1}. Compare also: c) C. J. Cramer, F. J. Dulles, G. J. Giesen, J. Almlöf, *Chem. Phys. Lett*. **1995**, *245*, 165 – 170; d) E. Goldstein, B. Beno, K. N. Houk, *J. Am. Chem. Soc.* **1996**, *118*, 6036 – 6043. An ancillary observation: the fact that the DFT hypersurface curvature reflects the features of the triplet surface may have some consequences when a bond formation process is considered between "C•" and "O•" centers in the diradicals (as in the cycloaddition pathway), because the repulsive nature of the triplet may introduce an 'excess of positive curvature', and raise the barrier.

[48] a) M. W. Wong, M. J. Frisch, K. B. Wiberg, *J. Am. Chem. Soc.* **1991**, *113*, 4776 – 4782; M. W. Wong, K. B. Wiberg, M. J. Frisch, *J. Chem. Phys.* **1991**, *95*, 8991 – 8998; M. W. Wong, K. B. Wiberg, M. J. Frisch, *J. Am. Chem. Soc.* **1992**, *114*, 523 – 529; J. B. Foresman, T. A. Keith, K. B. Wiberg, J. Snoonian, M. J. Frisch, *J. Phys. Chem.* **1996**, *100*, 16098 – 16104; b) L. Onsager, *J. Am. Chem. Soc.* **1936**, *58*, 1486 – 1493; J. G. Kirkwood, *J. Chem. Phys.* **1934**, *2*, 351 – 361; c) S. Miertus, E. Scrocco, J. Tomasi, *Chem. Phys.* **1981**, *55*, 117; S. Miertus, J. Tomasi, *Chem. Phys.* **1982**, *65*, 239; R. Cammi, J. Tomasi, *J. Chem. Phys.* **1994**, *100*, 7495 – 7502.

[49] GAUSSIAN98: M. J. Frisch, G. W. Trucks, H. B. Schlegel, G. E. Scuseria, M. A. Robb, J. R. Cheeseman, V. G. Zakrzewski, J. A. Montgomery, Jr., R. E. Stratmann, J. C. Burant, S. Dapprich, J. M. Millam, A. D. Daniels, K. N. Kudin, M. C. Strain, O. Farkas, J. Tomasi, V. Barone, M. Cossi, R. Cammi, B. Mennucci, C. Pomelli, C. Adamo, S. Clifford, J. Ochterski, G. A. Petersson, P. Y. Ayala, Q. Cui, K. Morokuma, D. K. Malick, A. D. Rabuck, K. Raghavachari, J. B. Foresman, J. Cioslowski, J. V. Ortiz, B. B. Stefanov, G. Liu, A. Liashenko, P. Piskorz, I. Komaromi, R. Gomperts, R. L. Martin, D. J. Fox, T. Keith, M. A. Al-Laham, C. Y. Peng, A. Nanayakkara, C. Gonzalez, M. Challacombe, P. M. W. Gill, B. Johnson, W. Chen, M. W. Wong, J. L. Andrei, M. Head-Gordon, E. S. Replogle, J. A. Pople, Gaussian, Inc., Pittsburgh, PA, **1998**.

[50] A. E. Reed, R. B. Weinstock, F. Weinhold, *J. Chem. Phys.* **1985**, *83*, 735 – 746; A. E. Reed, F. Weinhold, *J. Chem. Phys.* **1983**, *78*, 4066 – 4073; J. P. Foster, F. Weinhold, *J. Am. Chem. Soc.* **1980**, *102*, 7211 – 7218.

[51] K. Andersson, M. R. A. Blomberg, M. P. Fülscher, G. Karlström, R. Lindh, P.-Å. Malmqvist, P. Neogrády, J. Olsen, B. O. Roos, A. J. Sadlej, M. Schütz, L. Seijo, L. Serrano-Andrés, P. E. M. Siegbahn, P.-O. Windmark, MOLCAS Version 4, University of Lund, Sweden, **1997**.

[52] MolMol 2.4. A graphic program developed by the Institut für Molekular-biologie und Biophysik, EHT Zurich Spectrospin AG, Faellenden, Switzerland; R. Koradi, M. Billeter, K. Wüthrich, *J. Mol. Graphics* **1996**, *14*, 51 – 55.

[53] It is common practice to perform single-point calculations at a higher theory level on geometries optimized at a lower level. This results in probing the higher-level energy hypersurface in a somewhat arbitrary way. The overall reaction pathway on one surface, and the TS location along it, could be to some extent displaced with respect to their counterparts on the other surface. Therefore, in the CASPT2 energy difference estimations, a "geometrical factor" is intermingled with dynamical correlation effects.

[54] In the peroxirane-like second order saddle point, the first eigenvector (CASSCF frequency $646i\,cm^{-1}$) is dominated by the distance between the midpoint X of the C–C bond and the closer oxygen (O^1), coupled with the O–O bond length. The second eigenvector (CASSCF frequency $423i\,cm^{-1}$) is approximately directed toward the transition structure for diradical formation, and its principal component is the CXO^1 angle.

[55] F. Sevin, M. L. McKee, *J. Am. Chem. Soc.* **2001**, *123*, 4591 – 4600.

[56] R. Seeger, J. A. Pople, *J. Chem. Phys.* **1977**, *66*, 3045 – 3050.

[57] R. Bauernschmitt, R. Ahlrichs, *J. Chem. Phys.* **1996**, *104*, 9047 – 9052.

[58] H. B. Schlegel, J. J. McDouall, in *Computational Advances in Organic Chemistry* (Eds.: C. Ogretir, I. G. Csizmadia), Kluwer Academic, The Netherlands, **1991**, p 167.

[59] F. Motta, *Tesi di Laurea*, Università di Torino, July **2000**, pp. 42 – 47.

[60] R. D. Ashford, E. A. Ogryzlo, *J. Am. Chem. Soc.* **1975**, *97*, 3604 – 3607.

Received: October 22, 2002 [F4522]

